Evaluating Sensor Algorithms to Prevent Kitchen Cooktop Ignition and Ignore Normal Cooking

Amy Mensch, Anthony Hamins, Z.Q. John Lu, Matthew Kupferschmid, Wai Cheong Tam, and Christina You
National Institute of Standards & Technology
Gaithersburg, MD 20899-8664

Background

Cooking equipment is involved in nearly half of home fires in the USA, with cooktop fires the leading cause of deaths and injuries in cooking-related fires [1]. While new electric-coil cooktops must pass the UL[1] 858 [2] "abnormal cooking test," which aims to prevent cooktop fires, there is no such requirement for older and other types of cooktops. In this study, we considered the use of gas and particle sensors to provide early warning and/or stop cooktop ignition of foods and oils. Thus, the objective of this study is to find new, data-driven ways to reduce the risk of cooktop fires. Our approach is to develop and test the performance of sensor-detection algorithms using threshold analysis and machine learning methods.

Experimental Methods

Measurements were made in a mock kitchen using both electric and gas cooktops. There were four different burners used in the experiments: the small 15 cm diameter electric coil heating element with a measured power of 1.1 kW, the large 20 cm diameter electric coil heating element with a measured power of 1.8 kW, the medium gas burner with an estimated heat output of 3.4 kW, and the large gas burner with an estimated heat output of 4 kW. Sensors were placed in the exhaust duct above the cooktop and exposed to the gases and particles representative of cooking.[2] The flow in the exhaust duct (15 cm diameter) was characterized using a velocity probe placed in the center of the duct about 20 diameters downstream of a bend. The typical average velocity was 3.4 m/s with a standard uncertainty of ± 0.1 m/s. The average velocity varied between experiments with a standard deviation of 0.2 m/s. Using the electric coil cooktop, the duct temperature increased by an average of 9 °C causing an estimated reduction in duct mass flow of 3 %. For the gas cooktop, the duct temperature increased by an average of 23 °C, which is estimated to reduce the duct mass flow by 7 %. Additional details of the experimental apparatus and methods are described in Ref. [3].

A previous series of electric-coil element cooktop experiments in the same mock-up kitchen monitored sensor performance during the heating of vegetable oils, water, hamburgers, and salmon [3]. Many of the oil experiments and one salmon experiment led to ignition. The data from those experiments were supplemented with data from additional ignition and normal cooking experiments covering a wide range of conditions. The additional experiments, described in Table 1, included cooking bacon, french fries, and chicken. For a few experiments, multiple pans were heated on separate burners simultaneously. Some experiments were conducted using a gaseous (methane) fueled cooktop. In total, 39 of the 60 experiments led to ignition of the oil or food.

---

[1] Underwriters Laboratories
[2] Future experiments will consider the effects of sensor placement, ventilation, and configuration.

Table 1 Conditions for Experiments Augmenting Ref. [3]

Ignition	Heating Source	Pan Type	Pan Diameter	Food and Amount
N	electric coil	none	N/A	N/A
Y	electric coil	cast iron	20 cm	50 mL canola oil & 2 L water on separate burners
N	electric coil	cast iron & aluminum	20 cm	50 mL canola oil in each pan
N	electric coil	cast iron	20 cm	282 g chicken legs (2), 200 mL canola oil
Y	electric coil	cast iron	25 cm	223 g frozen french fries, 500 mL canola oil
N	electric coil	cast iron	25 cm	220 g bacon (8 slices)
Y	electric coil	cast iron	20 cm	110 g bacon (4 slices)
Y	electric coil	cast iron	20 cm & 25 cm	50 mL & 100 mL canola oil in separate pans
Y	electric coil	cast iron	20 cm & 25 cm	50 mL & 100 mL olive oil in separate pans
N	methane	none	N/A	N/A
Y	methane	cast iron	25 cm	100 mL canola oil
N	methane	cast iron	25 cm	N/A
Y	methane	cast iron	20 cm	50 mL canola oil
N	methane	cast iron	20 cm & 25 cm	50 mL & 100 mL canola oil in separate pans

Pan Temperature Measurements

In each experiment pan temperatures were measured at one or more locations using Type-K thermocouples either spot welded or peened to the top surface of the pan. The thermocouples showed significant variations in temperature across the pan surface. The standard uncertainty of the Type-K thermocouples was ± 3 °C. Figure 1 shows calibrated infrared (IR) images of dry (no oil) cast iron pans. The images reveal the distribution of temperature on the small electric coil element and on the large gas burner, which was influenced by pan orientation and geometry. The maximum temperature the camera could monitor was 370 °C, so regions above that temperature are shown as white. The simultaneous thermocouple measurements that were used to calibrate the IR images are labeled in the figure. From the thermocouple calibrations, the pan emissivity ranged from 0.88 to 0.96, depending on the experiment. The uncertainty in the IR temperatures was ± 8 °C. Figure 2 shows the pan surface thermocouple measurements during an experiment that led to ignition of canola oil. These figures demonstrate that temperature variation across the pan's bottom surface could reach 50 °C.

Figure 2 shows that the time series of the pan center temperature lagged temperatures measured toward the edge of the pan. Because the hottest region of the pan is where ignition is most likely, the maximum temperature was estimated in experiments when only the center pan temperature was measured. The estimate was based on a linear regression relationship between the thermocouple readings at the pan center and at the edge locations: 5 cm from the center in the 20 cm diameter cast iron pans, and 6 cm or 7.5 cm from the center in the 25 cm diameter cast iron pans. The linear regression relationships for the edge temperatures are shown in Table 2 as a function of center temperature for similar experiments (same pan size and burner size).

The average pan temperature at the time of ignition for all the experiments was 429 °C with a standard deviation of 25 °C. For the electric coil experiments, the maximum pan temperature at the time of ignition was between 403 °C and 483 °C. For the gas cooktop, the ignition temperatures of the pan were lower, between 371 °C and 382 °C. The gas cooktop also took much longer to ignite. The average time to ignition was 536 s for the 25 cm pan on the large electric coil burner and 1104 s for the 25 cm pan on the large gas burner. Heating a pan represents a complex set of heat transfer processes involving radiation, convection and conduction, and the burner and pan configurations play an important role. Consistent with the slower temperature rise for the gas cooktop, ignition was not observed on the 20 cm cast iron pan with 50 mL of canola oil using the medium gas burner. For the 20 cm cast iron pan with 50 mL of oil, ignition occurred only when the pan was placed on the large gas burner.

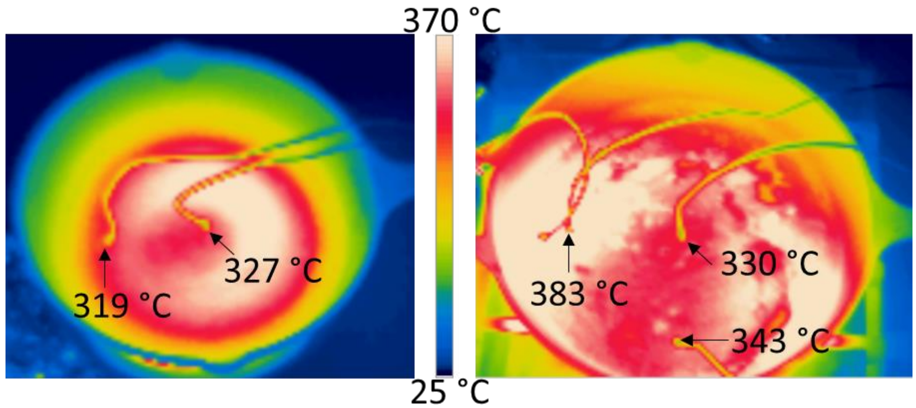

Figure 1. IR images showing the distribution of surface temperature of a 20 cm diameter cast iron pan heated by the small electric coil heating element (left) and the large gas burner (right).

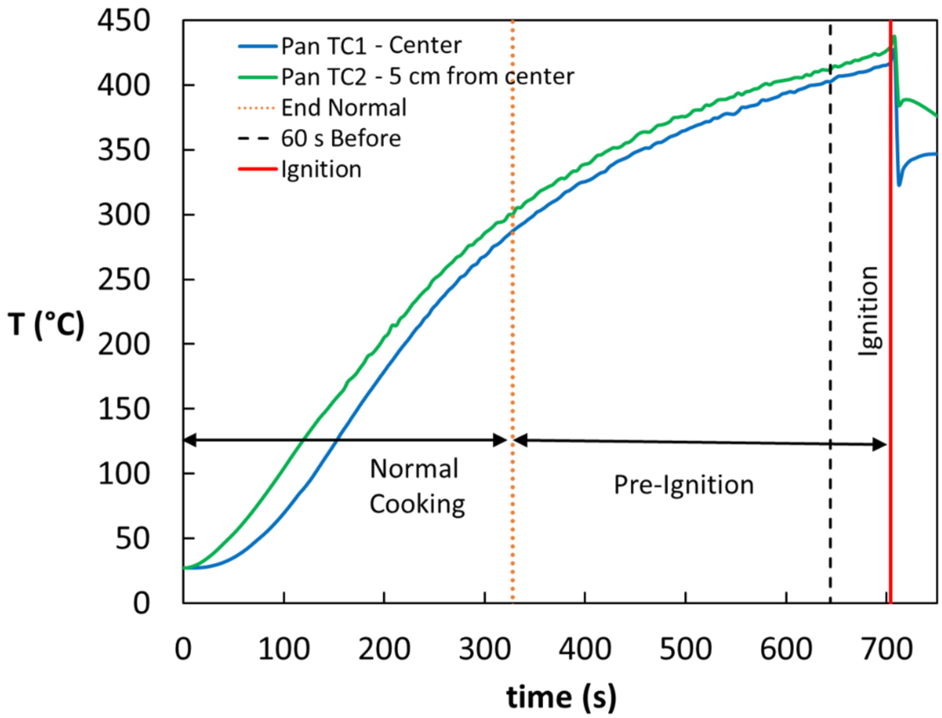

Figure 2. Pan surface temperatures and cooking regimes for an experiment leading to ignition of 50 mL of canola oil in a 20 cm diameter cast iron pan on the small electric coil heating element.

Table 2 Relationships Between Pan Thermocouple Temperatures

Experiment Type	Linear Regression	R^2
Electric coil, cast iron 20 cm pan, small burner	T_{5cm} = 0.972 T_{center} + 23 °C	0.99
Electric coil, cast iron 25 cm pan, small burner	T_{6cm} = 1.07 T_{center} + 16 °C	1.00
Methane, cast iron 25 cm pan, large burner	$T_{7.5cm}$ = 0.967 T_{center} + 31 °C	0.99

Defining Normal Cooking

To develop an algorithm that predicts ignition, normal cooking must be defined. This is because sensor performance involves not only quantifying the rate of missed ignitions, but also the rate of false alarms. A missed ignition means a candidate algorithm would not have been triggered before ignition. To ensure there would be enough time for the algorithm to intervene and prevent ignition, the thermal lag of the cooktop and burner-pan system must be considered. Previous work suggests that a period of 60 s before ignition is enough time to intervene and prevent ignition [4]. A false alarm means that the algorithm predicts ignition is imminent, but the conditions are that of normal cooking, and ignition is not likely.

Figure 2 illustrates three periods of a typical experiment: normal cooking, pre-ignition, and ignition. Initially, all experiments started as normal cooking. At some point, the conditions exceeded some reasonable temperature-based or time-based limit and transition to “pre-ignition.” Therefore, any condition that was not defined as normal cooking was labeled as pre-ignition, regardless of whether ignition eventually occurred later in the experiment. This was because the conditions during pre-ignition were considered beyond the requirements of normal cooking and potentially hazardous. Such conditions were accompanied by severely burned food and copious amounts of aerosol. The ignition period was defined as starting 60 s before ignition. Since there was no experiment in which the ignition period overlapped with normal cooking, it was possible for algorithms to predict ignition without interfering with normal cooking.

While the definition of the ignition period was straightforward, defining the reasonable limits of normal cooking required more nuance. The limits of normal cooking were based on either a maximum pan temperature, a safe food temperature, or the duration of cooking at an approximate pan temperature. For example, because the thickness of the vegetable oils and butter was thin (typically 3 mm), we assumed that the pan temperature gave a good indication of the oil temperature. When cooking foods such as meat, the pan temperature could be much hotter than the food, and food temperature was a better indicator of ignition potential than pan temperature. In defining normal cooking for meats, we took into account the USDA[3] safe minimum internal temperatures for chicken, 74 °C, fish, 63 °C, and ground beef, 71 °C [5].

The end of normal cooking for all types of oils and butter was defined when the pan temperature reached 300 °C. When deep-frying, it is recommended to keep oils below their smoke point, and the highest oil smoke points are around 230 °C [6]. Therefore, a limit of 300 °C allowed significantly more heating than recommended, while being well below oil ignition temperatures. For bacon, a USDA fact sheet states, “It’s very difficult to determine the temperature of a thin piece of meat such as bacon, but if cooked crisp, it should have reached a safe temperature.” [7]. Instead of relying on a “crispiness” determination, we treated bacon like oils, and the end of normal cooking was when the pan temperature reached 300 °C. This was reasonable since bacon is very high in fat, and liquid fat quickly coats the pan like vegetable oil. Photos taken at a pan temperature

[3] United States Department of Agriculture

of 300 °C showed that the bacon had already begun to blacken. Some bacon experiments led to ignition.

For chicken legs in 200 mL of preheated oil, the burner setting was on medium to maintain a pan temperature of about 200 °C for frying. The chicken legs were flipped every 4 min for a total cooking time of 18.5 min, which was 10 % longer than the time it took for the thermocouple inserted in the middle of the meat to reach 74 °C. This time was defined as the end of normal cooking, and the internal chicken temperature was 80 °C. For salmon fried in butter on high power for 4 min on each side, the thermocouples inside the meat did not show a steady increase in temperature. In most cases, the meat temperature exceeded 63 °C at least momentarily before the end of the 8 min of cooking, which was used as the end of normal cooking.

For hamburgers, the end of the frying procedure used by Cleary [8] was about 10 % longer than the time for the temperatures in the middle of the hamburgers to reach 71 °C. At the end of this procedure, the meat temperature was about 77 °C, which is an indication of well-done beef [9]. Therefore, the end of the frying hamburger procedure was defined as the end of normal cooking. For broiling hamburgers, the UL 217 Cooking Nuisance Smoke Test [10] specifies 25 min of broiling. However, in our experiments, adding an additional 10 % to the time when the hamburgers reached 71 °C, was less than 18 min (1122 s). This was defined as the end of normal cooking, and at this time the meat temperature was 82 °C.

For frozen fries in 500 mL of preheated oil, the burner power was adjusted periodically to maintain a pan temperature around 200 °C like was done for the experiments cooking chicken legs. There is no recommended safe temperature for fries, so the end of normal cooking was defined as 15 min of frying when the color of the fries had turned medium brown. After the end of normal cooking, the burner power was turned to high and the fries and oil later ignited.

Sensor Analysis

Sixteen sensors were positioned in the exhaust duct, approximately 3 m downstream of the range hood opening which was 0.8 m above the cooktop. The sensors monitored various quantities including CO_2, CO, temperature, humidity, smoke, hydrocarbons, alcohols, H_2, ammonia, natural gas, propane, volatile organic compounds (VOCs), and dust/aerosols. Raw data were acquired at 0.25 Hz. After each experiment, the average background signal for each sensor was subtracted from the raw signal output. Figure 3 plots the signals for a canola oil experiment on the gas burner, where the signals are normalized by the maximum value recorded from that sensor.

Sensor signal values and their ratios were evaluated to determine if a threshold value could be selected that both prevents ignition and ignores normal cooking conditions for all experiments. Machine learning was also used to develop algorithms to classify sensor data as representing normal cooking or pre-ignition conditions, and a similar performance metric was used. In addition to investigating the performance of thresholds of individual sensor values, we also considered the ratios between sensor values. CO_2 (PPM), duct temperature (K), and humidity (vol %) were used in the denominator of ratios. These signals did not include background subtraction to avoid dividing by zero because the values during the experiment were typically the same as the background.

Threshold Analysis

A threshold value of a sensor or sensor ratio could potentially miss ignitions as well as trigger false alarms. We considered the most conservative sensor or ratio threshold, which is the minimum value obtained at least 60 s before all ignitions. The false alarm rate to evaluate the threshold performance was defined as the ratio of the number of experiments with a false alarm to the total number of normal cooking experiments. Table 3 summarizes the results of the threshold analysis, listing the best performing sensors and sensor ratios. The operating principle of the signal (in the numerator for ratios) is also listed. The sensor name reflects manufacturer product literature, but a sensor could respond to other things as well. For example, the dust optical sensor operates using light scattering, which can occur for both dust particles and cooking aerosols. Most of the sensors are not calibrated, and therefore, only the threshold voltage is reported. The indoor air quality sensor outputs in arbitrary units of PPM.

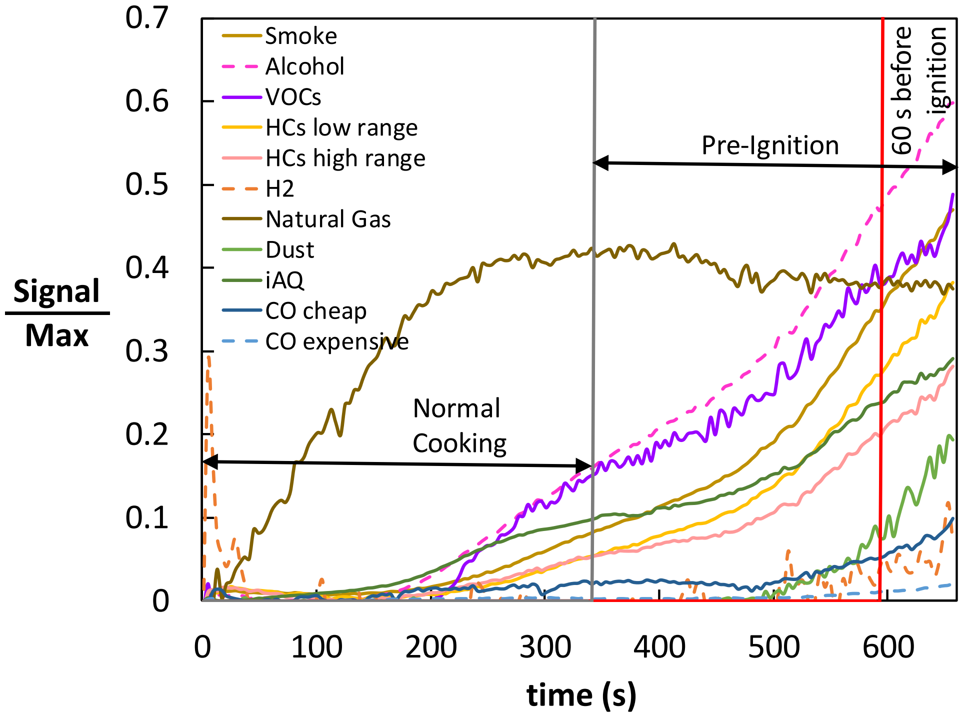

Figure 3. Sensor signals (background subtracted and normalized by sensor peak) and cooking regimes for an experiment leading to ignition of 50 mL of canola oil in a 20 cm cast iron pan on the large gas burner.

The best performance is for the volatile organic compounds (VOCs) sensor with a 2 % false alarm rate, or one false alarm in 60 experiments. The false alarm occurred about 2 min. before the end of normal cooking in one of the frying hamburger experiments with a 25 cm cast iron pan on the large electric coil burner. At that time, the thermocouples inside the hamburgers were both 68 °C, which is just below the safe temperature for ground beef (71 °C), but still within our definition of normal cooking. The ratios of sensors with duct temperature have similar performance to the sensor alone, but never better performance. One ratio that performs better than the sensor alone is the ratio of alcohol to humidity, which is slightly better than alcohol alone. A more significant improvement occurs for the ratio of the CO signals to CO_2, with the false alarm rate for the ratio of the expensive CO sensor nearly half of the CO sensor alone. The two different CO sensors both perform similarly despite the differences in output format (PPM vs. voltage) and price.

Table 3 Threshold Performance of Sensors and Select Sensor Ratio Pairs

Sensor	Threshold	Units	False Alarm Rate	Operating Principle
VOCs	0.57	V	0.02	metal oxide sensor
VOCs / Duct Temp.	0.0019	V/K	0.02	metal oxide sensor
iAQ	12000	PPM	0.06	electrochemical
iAQ / Duct Temp.	40	PPM/K	0.06	electrochemical
VOCs / Humidity	0.28	V/vol %	0.07	metal oxide sensor
Dust	0.20	V	0.08	optical
Dust / Duct Temp.	6.3E-04	V/K	0.08	optical
iAQ / Humidity	6100	PPM/vol %	0.09	electrochemical
Alcohol / Humidity	0.65	V/vol %	0.11	electrochemical
CO, expensive / CO_2	0.012	PPM/PPM	0.11	electrochemical
Alcohol	0.92	V	0.12	electrochemical
Alcohol / Duct Temp.	0.0030	V/K	0.12	electrochemical
Dust / Humidity	0.081	V/vol %	0.13	optical
CO, cheap / CO_2	2.2E-05	V/PPM	0.16	electrochemical
Dust / CO_2	1.53E-04	V/PPM	0.16	optical
CO, expensive	4.3	PPM	0.20	electrochemical
CO, cheap	0.0078	V	0.22	electrochemical
CO, cheap / Duct Temp.	2.6E-05	V/K	0.22	electrochemical
CO, expensive / Duct Temp.	0.014	PPM/K	0.22	electrochemical
CO, cheap / Humidity	0.0060	V/vol %	0.23	electrochemical
CO, expensive / Humidity	3.4	PPM/vol %	0.24	electrochemical
Hydrocarbons, low range	0.22	V	0.25	electrochemical
Combustible gas & smoke	0.41	V	0.27	electrochemical
Combustible gas & smoke / Duct Temp.	0.0013	V/K	0.27	electrochemical
H_2	0.15	V	0.28	electrochemical

Machine Learning Analysis

The sensor signals were also used to train a multi-layer perceptron neural network to develop a model that differentiates between normal cooking and pre-ignition conditions. TensorFlow[4] was used as the application program interface (API) to implement machine learning. Two hidden layers with 64 neurons and 32 neurons were activated with a rectified linear unit (ReLU) activation function. A sigmoid activation function was used to calculate the output. Each time point was treated individually with a classification label, which was assigned 0 within the normal cooking window and 1 during the pre-ignition period. The method considered over 12 800 time points in the 60 experiments.

[4] Certain commercial equipment, instruments, or materials are identified in this paper in order to specify the procedures adequately. Such identification is not intended to imply recommendation or endorsement by the National Institute of Standards and Technology, nor is it intended to imply that the materials or equipment identified are necessarily the best available for the purpose.

Using a cross-validation method, the neural network model was trained using the data from 59 experiments and then tested on the last experiment. This process was repeated 60 times until each experiment was excluded from the training and used once as the test set. The output for the test experiment was a value between 0 and 1 for each time point, which was the model prediction for the probability of pre-ignition. The values were rounded to 0 or 1 and the predictions were compared to the labels from the experiment within the normal cooking and the ignition (60 s before ignition) windows. The overall performance was evaluated by counting the number of normal cooking data sets with any wrongly predicted values of 1 (false alarms) and the number of ignition data sets with any wrongly predicted values of 0 (missed ignitions). Predictions between normal cooking and the ignition window were ignored.

The missed ignition rate is the number of ignitions missed by the prediction divided by the number of experiments in which ignition was observed ($n_{ignitions} = 39$). The false alarm and missed ignition rates are given in Table 4 for a baseline case and cases with only single sensor input. The baseline case used 11 sensor signals as input to the neural network. These included the sensors listed in Table 3 as well as an electrochemical hydrocarbon sensor with a higher range and an electrochemical natural gas sensor. Table 4 summarizes the results of the neural network analysis. The sensor operating principles are also listed. The performance of the single sensor input cases are listed in order of performance (after the baseline case). The missed ignition rates are low because the neural network was trained to predict pre-ignition, which begins well before the ignition window. The best performing sensors in Table 4 are similar to the sensors with good threshold performance. The baseline model performs worse than many of the individual sensors, but better than the performance of the worst individual sensors (e.g. natural gas false alarm rate was 0.57 and missed ignition rate was 0.38). The baseline performance was probably negatively affected by including input data from the poorest performing sensors.

Table 4 Neural Network Model Performance of Baseline and Single Sensor Cases

Input Data	**False Alarm Rate**	**Missed Ignition Rate**	**Operating Principle**
Baseline, 11 sensors	0.50	0	
Indoor air quality (iAQ)	0.24	0	electrochemical
Dust	0.26	0	optical
Volatile organic compounds (VOCs)	0.26	0	metal oxide sensor
Hydrocarbons, low range	0.28	0	electrochemical
CO, expensive	0.33	0	electrochemical
Alcohol	0.35	0	electrochemical
CO, cheap	0.35	0.03	electrochemical
Combustible gas & smoke	0.39	0	electrochemical
Hydrocarbons, high range	0.43	0	electrochemical
H_2	0.43	0.03	electrochemical
Natural gas	0.57	0.39	electrochemical

Conclusions and Future Work

Threshold analysis and machine learning analysis were used to estimate the performance of individual sensors with a false alarm rate that was similar for both types of analysis. A precise and consistent definition of normal cooking versus pre-ignition was required to evaluate that performance. To prevent ignition any algorithm must be triggered at least 60 s before ignition, which is defined as the ignition window. For the threshold analysis, the false alarm rate was reported for the threshold that was triggered before all ignition windows, so there were zero missed ignitions in every case. For the machine learning analysis, the rates of missed ignition were near zero since the neural network was attempting to detect pre-ignition, which began before the ignition window.

The performances of sensors with the lowest false alarm rates were in complete agreement between the two types of analysis. The best performing neural network models were based on sensors that also had good threshold performance. Although the machine learning false alarm rates were slightly higher than the threshold analysis, the initial neural network models were trained with only individual sensors as input. Future investigations of sensor performance will consider time-series effects to improve performance, such as evaluating sensor rate of change for threshold analysis and pre-processing input data to emphasize sensor rate of change for the machine learning analysis.

The combined information from multiple sensors was evaluated in a few limited cases: in sensor ratios with threshold analysis, and in the baseline neural network model with 11 sensor inputs. Some of the ratios performed as well as or better than the individual sensor values used in the ratios, but none of these cases performed better than the VOCs sensor alone. However, training neural networks with two or three sensors could provide an additional performance benefit by adding robustness and reliability to the model. Future work will involve combinations of two or three sensors as input data for neural network training, using the most promising sensors alone and in ratios: VOCs, iAQ, dust, CO, alcohol, duct temperature, humidity, and CO_2. The effects of transport conditions will also be considered.

[1] M. Ahrens, Home Fires Involving Cooking Equipment, National Fire Protection Association, Quincy, MA(2017).

[2] Underwriter's Laboratory, Northbrook, IL, Standard for Household Electric Ranges, Underwriter's Laboratory, Northbrook IL **UL 858** (2014).

[3] A. Mensch, A. Hamins, and K. Markell, Development of a Detection Algorithm for Kitchen Cooktop Ignition Prevention, *Suppression, Detection and Signaling Research and Applications Conference (SUPDET 2018)*, NFPA, Raleigh, NC(2018).

[4] E.L. Johnsson, Study of Technology for Detecting Pre-Ignition Conditions of Cooking-Related Fires Associated with Electric and Gas Ranges and Cooktops, Final Report, National Institute of Standards & Technology, Gaithersburg, MD(1998).

[5] Safe Minimum Internal Temperature Chart, United States Department of Agriculture, Food Safety and Inspection Service, https://www.fsis.usda.gov/safetempchart, (2019).

[6] Deep Fat Frying and Food Safety, United States Department of Agriculture, Food Safety and Inspection Service, https://www.fsis.usda.gov/wps/portal/fsis/topics/food-safety-education/get-answers/food-safety-fact-sheets/safe-food-handling/deep-fat-frying-and-food-safety/ct_index, (2013).

[7] Bacon and Food Safety, United States Department of Agriculture, Food Safety and Inspection Service, https://www.fsis.usda.gov/wps/portal/fsis/topics/food-safety-education/get-answers/food-safety-fact-sheets/meat-preparation/bacon-and-food-safety/ct_index, (2013).

[8] T.G. Cleary, A study on the performance of current smoke alarms to the new fire and nuisance tests prescribed in ANSI/UL 217-2015, National Institute of Standards and Technology, Gaithersburg, MD(2016).

[9] Meredith Home Group, Meat Temperatures Chart, https://www.marthastewart.com/270074/meat-temperatures-chart (2019).

[10] Underwriter's Laboratory, Northbrook, IL, Standard for Safety Smoke Alarms, **ANSI/UL 217** (2015).